Int J Clin Exp Med 2014;7(10):3253-3257
www.ijcem.com /ISSN:1940-5901/IJCEM0001998

Original Article

Differentiation of peripheral nerve functions and properties with spectral analysis and Karnovsky-Roots staining: a preliminary study

Qintong Xu[1], Zenggan Chen[1*], Qiong Li[1*], Haifei Liu[1], Jian Zhang[1], Wenhua Yao[3], Ren Zhang[3], Qingli Li[4], Hongying Liu[4], Feng Zhang[1], William C Lineaweaver[2]

[1]Department of Orthopedic Surgery, Zhongshan Hospital, Fudan University, Shanghai, China; [2]Joseph M. Still Burn and Reconstructive Center, Central Mississippi Medical Center, 1850 Chadwick Drive, Suite 1427 North Tower, 4 West Jackson, MS 39204; [3]Center of Analysis and Measurement, Fudan University, Shanghai, China; [4]Key Laboratory of Polar Materials and Devices, East China Normal University, Shanghai, China. [*]Equal contributors.

Received August 20, 2014; Accepted October 5, 2014; Epub October 15, 2014; Published October 30, 2014

Abstract: Objective: The purpose of this study was to explore the possibility for analyzing and differentiating between motor and sensory functions of peripheral nerve axons using spectral technology. Methods: 10 μm slide section of S1 anterior and posterior rabbit spinal nerve roots were made and then stained with Karnovsky-Roots method for molecular hyperspectral imaging microscopy analysis. In addition, Raman spectra data of nerve axons on each slide was collected after Karnovsky-Roots staining for 30 minutes. Results: Motor axons were differentiated from sensory axons in a nerve axon section hyperspectral image via Spectral angle mapper algorithm. Raman scatterings could be detected near 2110 cm^{-1}, and 2155 cm^{-1} in motor axons after Karnvosky-Roots staining. The value of I_{2100}/I_{1440} in motor axons are significantly different (P0.001) than in sensory axons after staining for 30 minutes. Conclusions: Motor and sensory nerve axons can be differentiated from their counterparts in 30 minutes by using Raman micro-spectroscopy analysis assisted with Karnovsky-Roots staining.

Keywords: Peripheral nerve, molecular hyperspectral imaging, Raman spectroscopy

Introduction

Peripheral nerve injury is one of the most common causes for deficiencies in motor and sensory functions leading to loss of labor. The repair and reconstruction of injured peripheral nerves has always been an important issue. One of the reasons for lacking efficacy of nerve repair is attributed to the mismatch of nerve stomp orientation and its motor and sensory components.

Cholinesterase staining is currently one of the most frequently used intra-operative methods in clinical practice. The Karnovsky-Roots staining protocol requires at least 8-12 hours for most AChE positive areas to properly manifest, which is time consuming and unsuitable for operation. Many surgeons have attempted to modify the formula to speed up the staining procedure. However, without enhancement in the basic principles, the sensitivity and specificity of the differentiation method remains unchanged.

The application of spectral analysis in medical science has been growing over recent years. Spectral technologies used in this study were molecular hyperspectral imaging (MHI) and Raman microspectroscopy. MHI integrates conventional imaging with spectroscopy and is capable of obtaining both spatial and spectral information from a specimen, a technique which enables investigators to analyze the chemical composition of traces while simultaneously visualize their spatial distributions [1]. MHI has already been applied in monitoring cancer [2], hemodynamics [3] and diabetic foot ulcers [4] as spectra of diseased cells deviated from their normal exhibitions. Preliminary research has already been successful regarding to the ability to describe nerve morphometry

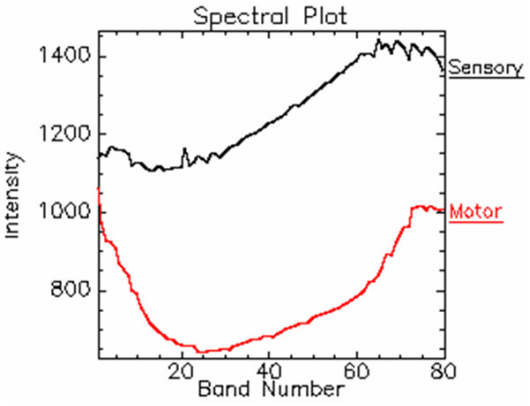

Figure 1. After Karnovsky-Roots staining, motor and sensory axons have different hyperspectral plots.

with MHI [5]. Raman microspectroscopy is a label-free method for rapid and sensitive detection of the status and changes in cells biomolecular microenvironments and is capable of both in vivo and ex vivo study. It has been used in detecting cancer cells [6], stem cells [7], inflammation [8], etc., based on recognizing specific Raman signatures expressed by certain radical groups.

We hypothesized that Karnovsky-Roots stained motor axons would exhibit different hyperspectral plots and Raman spectra from their sensory counterparts since the staining process would alter the chemical composition of the samples and generate its own unique spectral signals. The purpose of this study aimed to take advantage of the qualitative analyzing attributes of spectral technologies to identify and differentiate between motor and sensory functions and histological properties of peripheral nerve axons.

Methods

Twenty New Zealand rabbits (ordinary grade, 2.5 kg, random sex) were sacrificed through venous air injections for the bilateral harvest of their S1 anterior and posterior spinal nerve roots which strictly contained either motor or sensory peripheral nerve axons.

Three random samples from both anterior and posterior groups were separately cryosectioned into 10 μm thick slides with CM1850 cryostat (Leica, Germany), Karnovsky-Roots stained for four hours and viewed under a custom assembled molecular hyperspectral imaging system (Li, et al. [9], magnification 40x) with ENVI 4.0 software (Exelis, USA). Fifteen regions of interest (ROI) of motor and sensory axons and myelin sheaths were manually drawn over each gathered image to acquire their respective hyperspectral curves for computer analysis. Spectral angle mapper (SAM) algorithm was used to differentiate between the two kinds of nerve fibers and their sheaths.

Twenty anterior and twenty posterior root samples were randomly chosen and made into 30 μm frozen sections. Sections of every sample were scanned with Raman micro-spectroscopy (HORIBA Jobin Yvon LabRam-1b, 633 nm laser, 4.3 mW, 400 × magnification, France) after 30 minutes of conventional Karnovsky-Roots staining. For each slide, a blank background was also scanned. Raman spectra acquisition range was set for 400 cm^{-1} to 2400 cm^{-1} and time for 50 s. Raman spectra data were manually adjusted to eliminate background noise and florescence peaks in Labspec 3.0 (ASD, USA) by a single experienced Raman technician. Independent samples t-test was performed on I_{2100}/I_{1440} values of each slide with SPSS 19.0 (IBM, USA). A classification algorithm was formulated from the statistic results and was put to use in a diagnostic test performed with the remaining twenty anterior and twenty posterior spinal nerve roots, comparing our method against anatomical proof which was considered as “the golden standard”. Raman spectra were drawn with OriginPro 7.5 (Microcal, USA).

The staining protocol adopted in our study was the conventional Karnovsky-Roots acetylcholinesterase staining method. The incubation solutions were created and mixed 30 minutes before staining in the following order: 0.1 M Acetylthiocholine iodide 20 ml, 0.1 M pH = 6.5 phosphate buffer 160 ml, 0.1 M sodium citrate 10 ml, 30 mM copper sulfate 25 ml, 5 mM potassium ferricyanide. Staining was completed under room temperature.

Results

Karnovsky-Roots stained motor and sensory hyperspectral plots had respective characteristics (**Figure 1**). They were somewhat different and were able to be distinguished with ENVI’s Spectral Angle Mapper and shown on synthesized false-color images over the original section images (**Figure 2**).

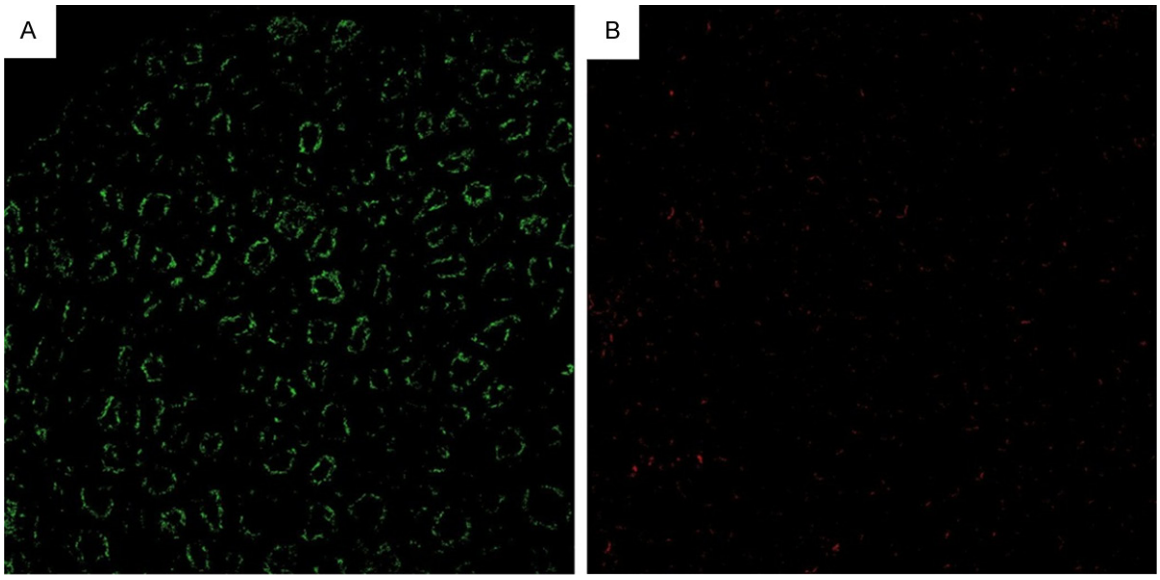

Figure 2. Using motor axons' average hyperspectral plot as standard and spectral angle mapper (α = 0.2) as algorithm, pixels with similar hyperspectral plots are differentiated and showed in false-color over the original images of motor and sensory nerve sections. Most motor axons were identified (A) and sensory axons were discarded (B).

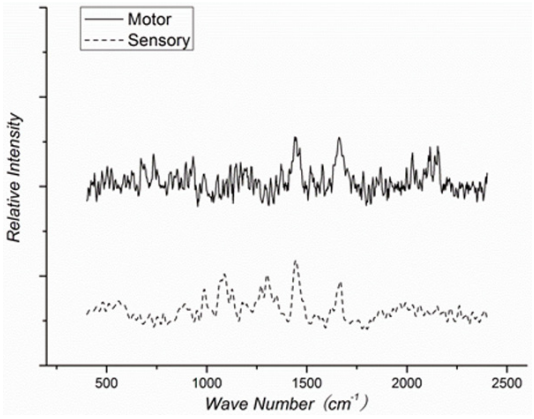

Figure 3. Comparisons between Raman spectra of Karnovsky-Roots stained motor axon (line) and sensory axon (dotted). Spectra of motor axon exhibits Raman peaks in 2100 cm^{-1} and 2155 cm^{-1}.

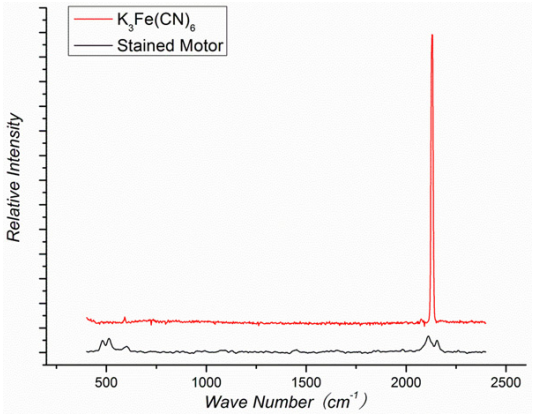

Figure 4. Comparisons between Raman spectra of Karnovsky-Roots stained motor axon (black) and incubation solution component potassium ferricyanide (red). CN has its characteristic frequency in 2100 cm^{-1} to 2160 cm^{-1} and is significant in motor axons' Raman spectra.

Raman spectra of motor axons showed Raman peaks in 2100 cm^{-1} and 2155 cm^{-1} whereas spectra of sensory axons remained near baseline value (**Figure 3**). We defined I_{2100} and I_{1440} as the maximum value of Raman scatterings in respectively 2100 cm^{-1} to 2160 cm^{-1} and 1425 cm^{-1} to 1455 cm^{-1}. The value of quotient I_{2100}/I_{1440} was analyzed with independent sample t-test. The average I_{2100}/I_{1440} was higher (t = -0.606, p0.05) in motor spectra (1.54 ± 1.11) than in sensory spectra (0.03 ± 0.03). ROC curve was calculated and cut-off point was between 0.17 and 0.33, where sensitivity and 1-specificity were respectively 1 and 0 at 0.17, 0.95 and 0 at 0.33. Therefore we chose an intermediate one-digit decimal of 0.2 as the cut-off.

Based on our criterion of classification, the Raman spectrum of any nerve axon would have to have a value of I_{2100}/I_{1440} higher than 0.2 to be classified as motor. Twenty anterior and twenty posterior nerve root samples were committed in a diagnostic test comparing quick staining and spectral analysis method against

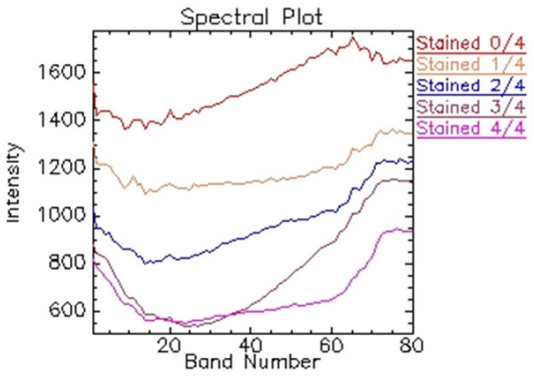

Figure 5. Hyperspectral plots of Karnovsky-Roots stained motor axons. Unstained motor axons exhibit an "S" shaped hyperspectral plot and through the increase of stain intensity the plot gradually became "U" shaped while the intensity values decreased.

the golden standard of anatomical/histological characteristics which suggest anterior roots be comprised of motor nerves and posterior roots of sensory nerves. All twenty anterior roots and nineteen posterior roots were correctly identified. One posterior root was false-positive. The sensitivity, specificity and accuracy of our method were 100%, 95%, and 97.5%, respectively.

Discussion

In hyperspectral imaging, myelin sheaths and nerve axons had very different hyperspectral plots and were easily identified with Spectral Angle Mapper (SAM). SAM is an algorithm that compares the cosine values between two spectral plots and determines whether they were similar or not. Our finding of myelin sheaths' distinct plots would be useful for histological and pathological studies as MHI may negate the need for myelin staining (i.e. Sudan black, Luxol blue, silver or potassium dichromate) which are extremely time-consuming and return with low specificity and contrast.

The stain intensities are not always equal in motor nerve fibers. Therefore, the hyperspectral plots of stained motor axons may vary in a certain pattern. As shown in **Figure 5**, unstained motor axons exhibit an "S" shaped hyperspectral plot and through the increase of stain intensity the plot gradually became "U" shaped while the intensity values decreased in motor axons. Because SAM compares two plots rather than two groups of plots, taking one as standard and the other as trial, SAM may not be the most ideal algorithm under such circumstance. A custom programmed algorithm which is capable of selecting multiple standard plots would likely be further preferred in order to gain exaltation for more accurate classification.

In our previous experiments using Raman spectroscopy, we had concurred with Wang et al. [10] that the Raman spectra of peripheral nerve axons both motor and sensory presented Raman signals near 1080 cm^{-1}, 1280 cm^{-1}, 1440 cm^{-1} and 1660 cm^{-1}, with 1440 cm^{-1} peak being strongest [11]. However, we did not find any significant differences between the two types of Raman spectra. We believed that differentiation of nerve properties should be based on distinct diversities rather than subtleness. Karnovsky-Roots staining if considered on a molecular scale is in fact copper ferrocyanide oxidized by acetylcholinesterase harbored in motor axons. By using Karnovsky-Roots staining as a spectral marker, we would in theory be able to locate characteristic frequencies of copper, ferrous and cyanide molecules or radicals in the Raman spectra of motor axons. Through experimentation, only CN frequencies in 2100 cm^{-1} to 2160 cm^{-1} turned out apparent after thirty minutes of staining (**Figure 4**). Such manifestation proved sufficient to be used as differentiation standard between motor and sensory properties.

One single false-positive result can be explained by non-specific staining of butyrocholinesterase (BuChE). Posterior spinal nerve roots contain a small amount of unmyelinated C fibers which appear scattered between the myelinated fibers in a spot or fleck form. Unmyelinated C fibers exhibit BuChE activity and are more intensely stained than myelinated fibers' AChE under the same circumstance [12]. It has been reported that iso-OMPA can suppress BuChE staining and can be added to staining process if higher specificity is desired [13].

There were limitations in our study. First, we were unable to avoid sample collection and sectioning, although this was merely an attempt to test whether spectral analysis was capable of differentiating similar cells with different functions. Secondly, only rabbit spinal nerve roots were used as specimen as they consisted mostly of either motor or sensory axons. Under such unification, a nerve sample would represent any single one of its axons. Human periph-

eral nerve samples are either mixed or sensory nerves. Therefore, any effort made to recognize and match a single specifically targeted axon from an entire nerve cross section would have been overwhelmed. In further studies, we plan to test our algorithms in mixed nerves under Raman spectral imaging systems.

In conclusion, we have made preliminary efforts in differentiation of motor and sensory nerve axons via Raman spectroscopy and hyperspectral imaging. Staining was conducted for four hours before MHI could properly detect motor spectra, and thirty minutes for Raman spectroscopy. These findings provide evidence for further investigation of utilizing spectral analysis to identify nerve fascicle properties and hopefully could achieve in situ spectral identification and differentiation.

Acknowledgements

The manuscript was sponsored by the Scientific Research Foundation for the Returned Overseas Chinese Scholars, State Education Ministry (2009), the Key Project grant of Shanghai Municipal Science and Technology Commission, (2010, Grant No. 10411953900) and National Natural Science Foundation of China (8120-1476).

Disclosure of conflict of interest

None.

Address correspondence to: Zeng-Gan Chen, Department of Orthopedic Surgery, Zhongshan Hospital, Fudan University, Shanghai, China. E-mail: chen.zenggan@zs-hospital.sh.cn; Qiong Li, Department of Orthopedic Surgery, Zhongshan Hospital, Fudan University, Shanghai, China. E-mail: liqiongtongxue@163.com

References

[1] Edelman GJ, Gaston E, van Leeuwen TG, Cullen PJ, Aalders MC. Hyperspectral imaging for non-contact analysis of forensic traces. Forensic Sci Int 2012; 223: 28-39.

[2] Siddiqi AM, Li H, Faruque F, Williams W, Lai K, Hughson M, Bigler S, Beach J, Johnson W. Use of hyperspectral imaging to distinguish normal, precancerous, and cancerous cells. Cancer 2008; 114: 13-21.

[3] Skala MC, Fontanella A, Hendargo H, Dewhirst MW, Izatt JA. Combined hyperspectral and spectral domain optical coherence tomography microscope for noninvasive hemodynamic imaging. Opt Lett 2009; 34: 289-291.

[4] Nouvong A, Hoogwerf B, Mohler E, Davis B, Tajaddini A, Medenilla E. Evaluation of diabetic foot ulcer healing with hyperspectral imaging of oxyhemoglobin and deoxyhemoglobin. Diabetes Care 2009; 32: 2056-2061.

[5] Li Q, Xu D, He X, Wang Y, Chen Z, Liu H, Xu Q, Guo F. AOTF based molecular hyperspectral imaging system and its applications on nerve morphometry. Appl Opt 2013; 52: 3891-3901.

[6] Wang H, Tsai TH, Zhao J, Lee AM, Lo BK, Yu M, Lui H, McLean DI, Zeng H. Differentiation of HaCaT cell and melanocyte from their malignant counterparts using micro-Raman spectroscopy guided by confocal imaging. Photodermatol Photoimmunol Photomed 2012; 28: 147-152.

[7] Harkness L, Novikov SM, Beermann J, Bozhevolnyi SI, Kassem M. Identification of abnormal stem cells using Raman spectroscopy. Stem Cells Dev 2012; 21: 2152-2159.

[8] Bi X, Walsh A, Mahadevan-Jansen A, Herline A. Development of spectral markers for the discrimination of ulcerative colitis and Crohn's disease using Raman spectroscopy. Dis Colon Rectum 2011; 54: 48-53.

[9] Li Q, Chen Z, He X, Wang Y, Liu H, Xu Q. Automatic identification and quantitative morphometry of unstained spinal nerve using molecular hyperspectral imaging technology. Neurochem Int 2012; 61: 1375-1384.

[10] Wang H, Ma F, Wang F, Liu D, Li X, Du S. Identification of motor and sensory axons in peripheral nerve trunk using immunohistochemistry and micro-Raman spectroscopy. J Trauma 2011; 71: 1246-1251.

[11] Xu Q, Chen Z, Zhang J, et al. Characteristics of microscopic structures in peripheral nerves under Raman spectroscopy and hyperspectral imaging. Chin J Clin Med 2013; 20: 245-248.

[12] Liu XL, Zhu JK. The histochemical study of rat sciatic nerve cholinesterase in degeneration and regeneration. J Reconstr Microsurg 1990; 6: 43-47.

[13] He YS, Zhang SZ. Acetylcholinesterase: a histochemical identification of motor and sensory in human peripheral nerve and its use during operation. Plast Reconstr Surg 1988; 82: 125-130.